

# Penetration depth study of anisotropic superconductivity in 2H-NbSe<sub>2</sub>

J.D. Fletcher,<sup>1</sup> A. Carrington,<sup>1</sup> P. Diener,<sup>2</sup> P. Rodière,<sup>2</sup>

J.P. Brison,<sup>2</sup> R. Prozorov,<sup>3</sup> T. Olheiser<sup>4</sup> and R.W. Giannetta<sup>4</sup>

<sup>1</sup> *H.H. Wills Physics Laboratory, University of Bristol, Tyndall Avenue, BS8 1TL, United Kingdom.*

<sup>2</sup> *CNRS-CRTBT, BP 166, 38042 Grenoble Cedex 9, France.*

<sup>3</sup> *Department of Physics and Astronomy and Ames Laboratory, Iowa State University, Ames, Iowa 50011.*

<sup>4</sup> *Department of Physics, University of Illinois at Urbana-Champaign, 1110 West Green St., Urbana, 61801 Illinois.*

(Dated: May 25, 2019)

We report measurements of the temperature dependence of both in-plane and out-of-plane penetration depths ( $\lambda_a$  and  $\lambda_c$  respectively) in 2H-NbSe<sub>2</sub>. Measurements were made with a radio-frequency tunnel diode oscillator circuit at temperatures down to 100 mK. The data show that there is a reduced energy gap on one or more of the quasi-two-dimensional Nb Fermi surface sheets. In contrast to some previous reports, we find that the gap on the Se sheet is at least as large as that on the Nb sheets.

The superconducting properties of the transition metal dichalcogenide compound 2H-NbSe<sub>2</sub> have been known for a long time to be unusual, with several features which cannot be explained by the conventional isotropic BCS model. There has been speculation that this is linked to the fact that the superconductivity emerges from a charge density wave state ( $T_{CDW} \simeq 33$ K) [1]. Recently, there has been renewed interest in this compound because of the possibility that it may be, like MgB<sub>2</sub> [2], a multigap superconductor (i.e., with distinct superconducting energy gaps on different Fermi surface sheets).

Evidence of significant gap anisotropy is found in heat capacity  $C$  measurements [3, 4]. The low temperature behavior of  $C$  ( $T \ll T_c$ ) is indicative of a small minimum gap ( $\sim 1k_B T_c$ ) and the non-linear increase in field of  $C$  [4] and thermal conductivity  $\kappa$  [5] suggests the presence of highly delocalized quasiparticles well below  $H_{c2}$ . Boaknin *et al.* [5] conclude that  $\kappa(H)$  is consistent with two distinct energy gaps on different Fermi surface sheets which differ by a factor  $\sim 3$ . A distribution of gap values, varying by a factor  $\sim 2$ , has also been observed in tunnelling measurements [6, 7].

In order to correctly interpret these experiments it is essential to have a good understanding of the normal state electronic structure. Electronic structure calculations within the local density approximation [8, 9] show that three bands cross the Fermi level giving rise to five Fermi surface sheets. Near the  $\Gamma$  point there is a small pancake like sheet which derives mostly from the Se  $p$  bands. This sheet should contributes only  $\sim 2\%$  to the in-plane superfluid density but  $\sim 80\%$  to the  $c$ -axis superfluid density (see Table I). The other four sheets derive from the Nb  $d$  bands and are weakly warped tubes running along the  $c$ -axis, centered either on the  $\Gamma$  or  $K$  points. The two surfaces derived from the bonding Nb  $d$  band are significantly more warped than those from the antibonding Nb  $d$  band.

This bandstructure has been found to be in good overall agreement with angle resolved photoemission spectroscopy (ARPES) [10, 11] and de Haas-van Alphen

(dHvA) measurements [9]. Significantly, the formation of the CDW state does not seem to lead to major Fermi surface reconstruction. dHvA measurements have only resolved signals originating from the small Se pancake and show that, although the shape is similar to band-structure calculations, its size is somewhat smaller. This reduces its contribution to the  $c$ -axis superfluid density by  $\sim 50\%$  [8]. The dHvA and ARPES results also show that mass renormalization factor ( $1 + \lambda_{m^*}$ ) varies considerably between sheets.  $\lambda_{m^*}$  is approximately 6 times larger on Nb sheet 17b than on the Se sheet 16 (see Table I).

There have been two experiments which have given  $\mathbf{k}$ -resolved information about the size of the superconducting energy gap  $\Delta(\mathbf{k})$ . Analysis of dHvA oscillations below  $H_{c2}$  have indicated that there is a relatively large energy gap on the Se pancake sheet,  $(1-2k_B T_c)$  [9]. Although the theoretical interpretation of the size of the additional damping in the superconducting state is far from straightforward [12] (especially in a multigap superconductor), the existence of a sizeable non-zero gap

TABLE I: Band structure estimates of the contribution of each Fermi surface (FS) sheet to the superfluid densities in each crystallographic direction ( $a, c$ ). The bare plasma frequencies  $\omega_P$  (in eV) from Ref. 8, are related to the renormalized superfluid densities by  $\rho = (\omega_P e/c\hbar)^2/(1 + \lambda_{m^*})$ , where  $\lambda_{m^*}$  is the mass renormalisation factor derived from dHvA measurements [9] (band 16) and ARPES [10] (bands 17 and 18). The numbers in parenthesis are the percentage contributions of each sheet to the total renormalized superfluid density.

FS Sheet	$\omega_{P,a}$	%	$\omega_{P,c}$	%	$\lambda_{m^*}$
16	0.4	(2)	2.16	(85)	0.3
17a	1.63	(25)	0.78	(8)	0.85
17b	1.65	(16)	0.86	(6)	1.9
18a	1.60	(24)	0.13	(0.2)	0.85
18b	1.85	(32)	0.26	(0.9)	0.85

would appear to be a robust feature of the data. ARPES measurements [11] on the other hand, have indicated that the gap on the Se sheet is very small (below  $0.16 k_B T_c$ ), whereas it is much larger ( $1.6 \pm 0.16 k_B T_c$ ) on the other four sheets. It should be mentioned however, that these latter measurements were performed at  $T = 5.3$ K, which is very close to  $T_c \simeq 7.1$ K

In an anisotropic superconductor the temperature dependent components of the superfluid density  $\rho = 1/\lambda^2(T)$  are sensitive to the distribution of the size of the superconducting gaps on the Fermi surface [13]. In this paper we present measurements of the temperature dependence of both the in-plane and  $c$ -axis magnetic penetration depths [ $\lambda_a(T)$  and  $\lambda_c(T)$ ] of  $\text{NbSe}_2$  from 100 mK up to  $T_c$ . Our data show that there is a reduced energy gap on one or more of the Nb Fermi surface sheets, but the gap on the Se sheet is not significantly smaller.

The temperature dependent part of the penetration depth was measured in single crystals of  $\text{NbSe}_2$  using a radio frequency (RF) resonant tunnel diode circuit [14]. The sample was attached with vacuum grease to a sapphire rod, the other end of which is attached to a temperature controlled stage. Changes in the resonant frequency of the circuit relative to the base temperature ( $\Delta F$ ) are directly proportional to changes in the field penetration in the sample. As the RF magnetic fields are very weak ( $\sim 10^{-5}$  T), and the dc field is screened with mu-metal to a similar level, we ensure the sample is always in the Meissner state. For  $H \parallel c$  the screening currents flow only in the basal plane and  $\Delta F = \alpha \Delta \lambda_a$ , where the geometric factor  $\alpha$  is estimated using the technique described in Ref. [15]. For  $H \perp c$  currents flow both in the plane and along the  $c$ -axis, and (neglecting the small contribution from the top and bottom faces) for a rectangular sample with dimensions  $l_x$ ,  $l_y$  and  $l_z$  [ $x,y$  are in-plane and  $l_x, l_y, l_z \gg \lambda$ ]  $\Delta F$  for  $H \parallel y$  is given by [15]:

$$\Delta F/\Delta F_0 = 2\Delta \lambda_a/l_z + 2\Delta \lambda_c/l_x. \quad (1)$$

Here  $\Delta F_0$  is the frequency shift obtained when the sample is completely removed from the coil and accounts for the sample demagnetizing factor as well as the coil calibration factor.

Measurements were conducted on samples from three different sources (Tsukuba, Lausanne, Bell labs) in three different laboratories. All samples were grown via the usual iodine vapor transport technique and are known to be of high quality, having a high  $T_c \simeq 7.1$ K and low residual resistances (RRR  $\simeq 40$ ). Some of the samples were from the same batch as those used for dHvA measurements [9]. Experiments in Bristol were performed in either a dilution fridge ( $T_{\min} \simeq 100$  mK) or a pumped  ${}^4\text{He}$  cryostat ( $T_{\min} \simeq 1.3$  K). In Grenoble and Urbana-Champaign a  ${}^3\text{He}$  cryostat was used ( $T_{\min} \simeq 0.5$  K). In total more than 15 samples were measured, several in both field orientations.

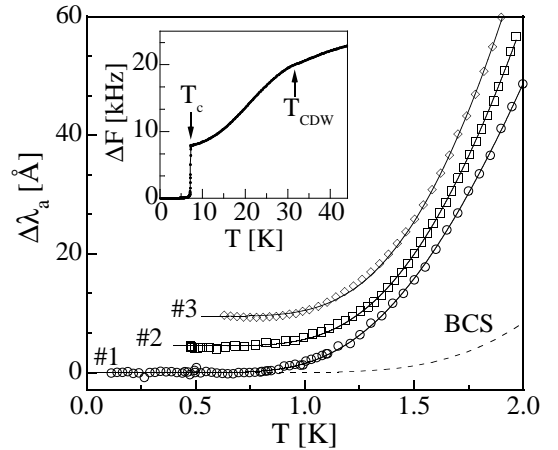


FIG. 1: Temperature dependence of the in-plane penetration depth,  $\Delta\lambda_a$  in single crystals of  $\text{NbSe}_2$ . Data for three different samples are shown. The absolute scale of  $\Delta\lambda_a$  is most accurate for sample 1 (see text). For samples 2 and 3 the data have been divided by 1.3 and 1.5 respectively and offset for clarity. Inset: Frequency shifts at higher temperature showing the charge density wave transition.

Fig. 1 shows the low temperature variation of the in-plane penetration depth data which probes mostly the excitations on the Nb sheets (see above). Data is shown for three samples measured in different laboratories. Sample 1 (Bristol) was very thin (aspect ratio  $\sim 40$ ) with  $H \perp c$ , hence the contribution from  $\Delta\lambda_c$  is negligible ( $< 2\%$ ), samples 2 (Urbana/Ames) and 3 (Grenoble) were thicker with  $H \parallel c$ . All three curves are fitted to the expression

$$\frac{\Delta\lambda}{\lambda(0)} \simeq \sqrt{\frac{\pi\Delta_0}{2T}} \exp\left(-\frac{\Delta_0}{T}\right), \quad (2)$$

which approximately reproduces the full solution to the BCS equations for  $T \lesssim T_c/3$ . For all samples we find  $\Delta_0 = 1.1 \pm 0.1 T_c$ . The data clearly show the presence of excitations with an energy gap much smaller than the weak coupling BCS value ( $\Delta_0 = 1.76 T_c$ ) on the quasi-2D Nb sheets of Fermi surface.

The temperature dependence of  $\Delta\lambda_a$  was very similar in all samples. The absolute values of  $\Delta\lambda_a$  measured with  $H \parallel c$  are consistently higher than those for  $H \perp c$  (in the opposite sense to that expected from the additional  $\lambda_c$  contribution for  $H \perp c$ ). It is likely that this results from the mica-like morphology of the crystals. Although very flat (001) faces may be prepared by cleaving, cutting the crystal perpendicular to this direction produces splintered edges which have a larger effective area than their geometric cross-section (and hence larger effective field penetration). For this reason, we believe the calibration factor is most accurately determined for the thin sample with  $H \perp c$  (sample 1 in Fig. 1) where  $\sim 98\%$  of the signal comes from the flat faces.

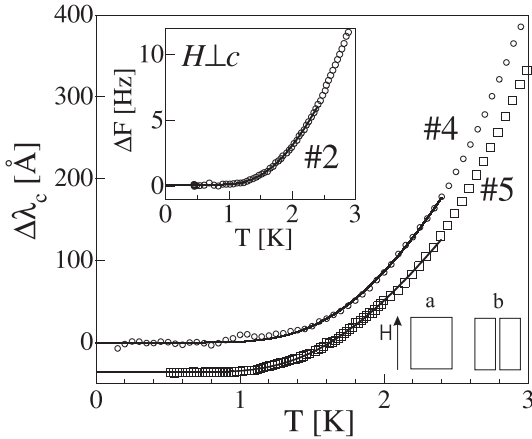


FIG. 2: Low temperature behavior of  $\Delta\lambda_c$  determined by cutting the sample (see text). Data for two different samples are shown. For sample 5 the data have been divided by 2 and offset for clarity. The solid line is a fit to Eq. 2 up to 2.4 K. The lower inset shows the geometry of the sample before and after cutting. Upper Inset: Raw measured frequency shift for a thick sample with  $H \perp c$  (same sample as #2 in Fig. 1).

Although the above in-plane data clearly shows the presence of a reduced gap on the Nb sheets it contains very little information about the gap on the Se sheet. If the gap on the Se sheet is significantly smaller than that on the Nb sheets we would expect the temperature dependence of  $\lambda_c$  to differ markedly from that of  $\lambda_a$ . We have investigated this in two ways. For thick samples, with  $H \perp c$  a significant proportion of the total measured  $\Delta F(T)$  comes from current running along the  $c$ -axis. In the inset to Fig. 2 we show data for a sample with aspect ratio ( $l_z:l_x \simeq 1:2$ ).  $\Delta F$  is temperature independent for  $T \lesssim 1.2$  K which clearly shows that the gap is not substantially smaller on the Se sheet than on the Nb sheets.

An alternative approach is to measure  $\Delta F$  with  $H \parallel x$  before and after cutting the sample in half along the field direction (see Fig. 2). In principle, the in-plane contribution is unchanged before and after cutting, so by subtracting the two frequency shifts we isolate the signal coming from the  $c$ -axis currents. In practice however, there could remain some contribution from  $\lambda_a$  because the effective edge area may change when the sample is cut due to splintering.

In the main part of Fig. 2 we show our result for the low temperature behavior of  $\Delta\lambda_c$  determined by the cutting method. The data are temperature independent below  $\sim 1.2$  K and a fit to Eq. 2 gives  $\Delta_0 = 1.3 \pm 0.1 T_c$  (the uncertainty reflects the changes in  $\Delta_0$  as the temperature fitting range is varied up to  $T_c/3$ ). This shows that the gap on the Se sheet is at least as large as that on the Nb sheets. The measured temperature dependence of  $\lambda_c$  is reproducible between the two samples measured but there is an uncertainty in its absolute magnitude (see figure).

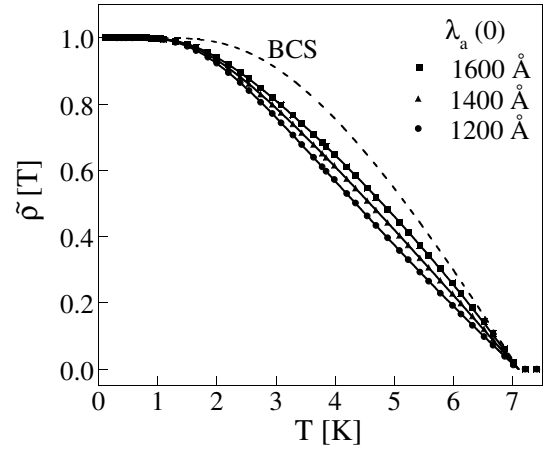


FIG. 3: Temperature dependence of the normalized in-plane superfluid density  $\tilde{\rho}_a$ . The solid symbols are  $\tilde{\rho}_a$  calculated from the measured  $\Delta\lambda_a(T)$  with the  $\lambda_a(0)$  values indicated. The solid lines are fits to the two gap model described in the text. The dashed line is the weak coupling BCS prediction with  $\Delta_0 = 1.76$  Å.

In order to proceed further with the analysis it is convenient to calculate the normalized superfluid density,  $\tilde{\rho} = \lambda(0)^2/\lambda(T)^2$ . From measurements of the reversible magnetisation in the vortex state [16] in some of the same samples shown above we find  $\lambda_a(0) = 1400 \pm 100$  Å. This is in reasonable agreement with muon spin rotation measurements [17] which give  $\lambda_a(0) = 1250$  Å.

We show in Fig. 3 the calculated in-plane  $\tilde{\rho}(T)$  for a range of values of  $\lambda_a(0)$  which encompass the experimental uncertainty. As the data clearly do not follow the standard BCS behavior we have attempted to model  $\rho_a(T)$  using a BCS approach with a  $\mathbf{k}$ -dependent gap. In the clean local limit BCS theory  $\rho_a$  is given by [13]

$$\rho_a(T) = \frac{\mu_0 e^2}{4\pi^3 \hbar} \left\{ \oint dS_F \frac{v_a^2}{v} + 2 \oint dS_F \frac{v_a^2}{v} \int_{\Delta_k}^{\infty} \frac{df(\varepsilon)}{d\varepsilon} \frac{\varepsilon}{(\varepsilon^2 - \Delta_k^2)^{\frac{1}{2}}} d\varepsilon \right\} \quad (3)$$

where  $dS_F$  is an element of Fermi surface,  $v$  is the Fermi velocity,  $f$  is the Fermi function and  $\Delta_k$  is the  $\mathbf{k}$  dependent energy gap.

Our first approach is to assume that there are different isotropic gaps on each of the two quasi-2D Nb bands (similar to the situation in  $\text{MgB}_2$ ) [18, 19, 20]. Eq. 3 then reduces to

$$\tilde{\rho}(T) = x\tilde{\rho}[T, \Delta_1(T)] + (1-x)\tilde{\rho}[T, \Delta_2(T)] \quad (4)$$

where  $x$  is the Fermi surface weight, which in the clean limit is proportional to  $\omega_{P,a}^2$  on each pair of sheets.  $\Delta_{1,2}(T)$  are assumed to have the BCS weak coupling temperature dependence but a variable low temperature amplitude. The fits to the data with this model are excellent (see Fig. 3). The parameters are given in Table

TABLE II: Variation of the fit parameters to models of the in-plane superfluid density, as a function of the assumed zero temperature value of  $\lambda_a$ .  $\Delta_1$ ,  $\Delta_2$ , and  $x$  are the parameters of the two-gap model (Eq. 4) and  $\Delta(0)$  and  $\epsilon$  are the parameters of the 6-fold anisotropic gap model (Eq. 5). The final line shows the parameters found by fitting the same models to the heat capacity  $C$  data of Ref. 4.

$\lambda_a(0)$	Two gap			6-fold gap	
	$\frac{\Delta_1}{T_c}$	$\frac{\Delta_2}{\Delta_1}$	$x$	$\frac{\Delta_{\min}(0)}{T_c}$	$\frac{1+\epsilon}{1-\epsilon}$
1200 Å	0.99	1.59	0.43	0.94	1.74
1400 Å	1.04	1.76	0.49	0.91	2.07
1600 Å	1.08	1.91	0.50	0.91	2.33
$C$	1.31	1.76	0.30	1.25	2.31

II. The value of the small gap varies little with  $\lambda_a(0)$  and is close to that found from fitting Eq. 2. The gap ratio is  $\Delta_2/\Delta_1 = 1.8 \pm 0.2$  and approximately 50% of the superfluid density resides on each pair of FS sheets.

As  $\text{NbSe}_2$  is hexagonal, another approach is to assume a gap with 6-fold symmetry on all Fermi surface sheets, which are approximated as simple tubes, i.e.,

$$\Delta(\phi, T) = \Delta_{\min}(T) \frac{[1 + \epsilon \cos(6\phi)]}{1 - \epsilon} \quad (5)$$

where as above  $\Delta_{\min}(T)$  is assumed to have the BCS temperature dependence and  $\phi$  is the in-plane angle. The fits to this model (not shown) are as good as for the two gap model above. The two free parameters [ $\Delta_{\min}(0)$  and  $\epsilon$ ], which vary slightly with the assumed  $\lambda_a(0)$ , are given in Table II. The ratio of the maximum to minimum gap  $(1 + \epsilon)/(1 - \epsilon) = 2.0 \pm 0.3$ , which is close to that found for the 2 gap fits.

By analyzing the zero field specific heat data of Ref. 4 with the same models [18] we find that the gap values are  $\sim 30\%$  higher than those from the superfluid density analysis, however the values of the gap anisotropy are very similar (see Table II) [21].

Usually, very high purity samples are required for any intrinsic gap anisotropy to be observed experimentally. More quantitatively the criterion for observing an anisotropic gap is [22]

$$\hbar\tau^{-1} \ll \sqrt{\langle\Delta\rangle\delta\Delta} \quad (6)$$

where  $\tau^{-1}$  is the impurity scattering rate,  $\langle\Delta\rangle$  is the average gap and  $\delta\Delta$  is its variation over the Fermi surface. Using the parameters of either the 6-fold anisotropic gap model or the two gap model yields  $\sqrt{\langle\Delta\rangle\delta\Delta} \simeq 7\text{K}$ . The residual resistance of our samples is typically  $\rho_0 = 2.8\mu\Omega\text{cm}$ . Assuming isotropic scattering, we can estimate the mean free path  $\ell = \mu_0 c^2 \hbar^2 v_a / (\omega_{P_a}^2 e^2 \rho_0) = 280\text{\AA}$ , and  $\hbar\tau^{-1} = \hbar v_a / (k_B \ell) \simeq 25\text{ K}$  (taking  $v_a$  as the average ARPES value[10]). This suggests that if the scattering

were isotropic then  $\tau^{-1}$  is  $\sim 4$  times too high for the gap anisotropy deduced from our models [23].

It seems then, unlikely that gap anisotropy within a single sheet could survive with this amount of scattering. However, reduced scattering between the two Nb bands (17 and 18) could allow two different gaps to exist on these pairs of FS sheets (as for  $\text{MgB}_2$  [24]). As the low temperature fit to  $\Delta\lambda_c$  gave a slightly larger value of  $\Delta_0$  it is likely that the smaller of the two gaps is on the band 18 Nb sheets as these should contribute very little to  $\lambda_c$ . A larger gap on band 17 is consistent with the larger value of  $\lambda_{m^*}$  found on sheet 17b.

In conclusion, our measurements of the anisotropic temperature dependence of the superfluid density in  $\text{NbSe}_2$  show evidence for two gap superconductivity, but in contrast to some previous reports, we argue that it is likely the smaller energy gap is located on the Nb sheets rather than on the Se sheet.

We thank I. Mazin and for useful discussions, as well as H. Berger, Y. Onuki and P. Gammel for providing the  $\text{NbSe}_2$  samples.

---

- [1] D. E. Moncton, J. D. Axe, and F. J. Disalvo, Phys. Rev. B **16**, 801 (1977).
- [2] A. Y. Liu, I. I. Mazin, and J. Kortus, Phys. Rev. Lett. **87**, 087005 (2001).
- [3] N. Kobayashi, K. Noto, and Y. Muto, J. Low Temp. Phys. **27**, 217 (1977).
- [4] D. Sanchez, *et al.*, Physica B **204**, 167 (1995).
- [5] E. Boaknin, *et al.*, Phys. Rev. Lett. **90**, 117003 (2003).
- [6] K. Iwaya, *et al.*, Physica B **329-333**, 1598 (2003).
- [7] J. G. Rodrigo and S. Vieira, Physica C **404**, 306 (2004).
- [8] M. Johannes, I. Mazin, and C. Howells, cond-mat/0510390 (2006).
- [9] R. Corcoran, *et al.*, J. Phys.-Condes. Matter **6**, 4479 (1994).
- [10] T. Valla, *et al.*, Phys. Rev. Lett. **92**, 086401 (2004).
- [11] T. Yokoya, *et al.*, Science **294**, 2518 (2001).
- [12] K. Yasui and T. Kita, Phys. Rev. B **66**, 184516 (2002).
- [13] B. S. Chandrasekhar and D. Einzel, Ann. Phys.-Leip. **2**, 535 (1993).
- [14] A. Carrington, R. W. Giannetta, J. T. Kim, and J. Giapintzakis, Phys. Rev. B **59**, R14173 (1999).
- [15] R. Prozorov, R. W. Giannetta, A. Carrington, and F. M. Araujo-Moreira, Phys. Rev. B **62**, 115 (2000).
- [16] Z. D. Hao, *et al.*, Phys. Rev. B **43**, 2844 (1991).
- [17] F. D. Callaghan, M. Laulainen, C. V. Kaiser, and J. E. Sonier, Phys. Rev. Lett. **95**, 197001 (2005).
- [18] F. Bouquet, *et al.*, Europhys. Lett. **56**, 856 (2001).
- [19] J. D. Fletcher, *et al.*, Phys. Rev. Lett. **95**, 097005 (2005).
- [20] F. Manzano, *et al.*, Phys. Rev. Lett. **88**, 047002 (2002).
- [21] For the  $C$  analysis  $x$  is proportional to the relative contribution of the density of states of each band to the total.
- [22] I. I. Mazin, *et al.*, Phys. Rev. B **69**, 056501 (2004).
- [23] T. Hanaguri, *et al.*, Physica B **329**, 1355 (2003); this work shows that  $C(H)$  is not strongly affected by impurities until the residual resistance ratio falls below  $\sim 40$ .

[24] I. I. Mazin, *et al.*, Phys. Rev. Lett. **89**, 107002 (2002).